Propagation of Nanopatterned Substrate Templated Ordering of Block Copolymers in Thick Films

L. Rockford,[†] S. G. J. Mochrie,[‡] and T. P. Russell*,[†]

Department of Polymer Science and Engineering, University of Massachusetts at Amherst, Amherst, Massachusetts 01002, and Department of Physics and Applied Physics, Yale University, New Haven, Connecticut 06520

Received October 10, 2000; Revised Manuscript Received December 15, 2000

ABSTRACT: Control over the orientation of a symmetric block copolymer lamellar morphology using a striped, chemically heterogeneous surface has been established. Films of symmetric diblock copolymers of poly(styrene-*block*-methyl methacrylate) solution cast onto silicon oxide substrates striped with periodic, 20 nm wide gold lines show lamellar microdomain orientation perpendicular to the substrate plane and parallel to the striping. Commensurability of the block copolymer and substrate stripe period is found to be essential to produce such a surface-directed morphology. A mismatch in length scale of only ±10% is sufficient to lose control over the microdomain orientation. This window of commensurability for thick films is much smaller than that found previously for ultrathin films. Consequently, more stringent conditions are met in unconfined films to direct the morphology with the surface. The distance over which the orientation of the microdomains persists is found to depend on the ordering kinetics, scaling with copolymer molecular weight, and is independent of the microdomain orientation at the surface.

Introduction

The use of block copolymers as templates for the fabrication of novel nanostructured materials has flourished due to the ease with which such templates can be prepared, and functionalized,[1−3] and to the variety of distinct nanostructures that can be generated from copolymer morphologies. Incorporation of these new materials into devices, however, is significantly hindered by the inability to control the self-assembly process that is the foundation of copolymer-based nanostructure synthesis. Microscopic grain sizes,[4] grain boundaries, and other defect structures[5] reduce the overall yield of the target nanostructure and prohibit real-space characterization and serial addressing of the nanoscopic domains. As a consequence, block copolymer morphologies at surfaces have been investigated with increasingly complex schemes in an effort to understand the effect of interfacial energy and confinement on the orientation of the microdomains. Such knowledge will facilitate the preparation of defect-free, oriented nanoscopic structures over large areas for use in future devices.

A basis for the control over the orientation of copolymer microdomains in thin films has already been established. Preferential interfacial interactions have been shown to impart an orientation of a lamellar morphology parallel to a surface, even above the ordering temperature.[6,7] Confinement of morphologies by film thickness has shown that the competition between enthalpy and entropy can be used to reorient the lamellar microdomains in ultrathin films,[8−11] produce a controlled roughness via island and hole formation at a thin film's free surface,[12] or induce tension and compression in copolymer morphology under one-dimensional confinement.[13] This understanding has enabled the design of experiments with more stringent control[14] in an effort to produce a desired morphology and orientation, and recent studies have established a strong precedent for surface or interface templated growth. Chemically[15] and topographically[16] patterned surfaces and static[17] and moving interfaces or phase boundaries[18] have all been used to control the orientation of nanostructures over large areas. Theoretical approaches[19−23] and simulations[24,25] have also indicated that, with the appropriate surface boundary conditions and processing procedures, lateral control over nanostructures may propagate microns away from a surface, providing true three-dimensional control over self-assembled nanostructures.[26] Here, we show experimental results demonstrating control over the lamellar morphology of a symmetric diblock copolymer, and discuss the limits over which such control can be achieved.

Previously, it was shown[15] that when solution cast on a chemically heterogeneous, flat surface comprised of 30 nm alternating stripes of nonpolar gold (Au) and polar silicon oxide (SiOx), a symmetric block copolymer of poly(styrene-*block*-methyl methacrylate), denoted P(S-*b*-MMA), ordered with the lamellar microdomains oriented normal to the surface and along the stripe direction. While confinement of the ultrathin films contributed to the perpendicular orientation of the lamellar microdomains, the strong coupling between the polar PMMA and SiOx on the substrate and the nonpolar PS and Au on the substrate produced an additional orientation of the domains parallel to the Au/SiOx stripes. The interactions between the blocks of the copolymer and the surface stripes were sufficiently strong to orient the morphology when there was as much as a 25% mismatch between the copolymer period and the substrate stripe period.

Here, experimental results are presented on thick copolymer films prepared on chemically heterogeneous surfaces, where confinement effects due to film thickness are removed. These experiments address the issue of whether the chemical heterogeneities of the substrate alone are sufficient to orient the block copolymer

[†] University of Massachusetts at Amherst.
[‡] Yale University.

10.1021/ma001747c CCC: $20.00
Published on Web 01/25/2001

Table 1. Summary of the Poly(styrene-*block*-methyl methacrylate) (S/MMA) Block Copolymers Used in Experiments; One Sample Possessed a Deuterated Methyl Methacrylate Block (dMMA)

coplymer	M_w (kg/mol)	period[a] L (nm)	δ for 42 nm substrate
S/MMA	53	27.38	0.65
S/MMA	73	33.71	0.80
S/MMA	84	36.93	0.88
S/MMA	107.8	43.22	1.03
S/MMA	113	44.78	1.07
S/dMMA	121.3	46.82	1.11
S/MMA	177	59.95	1.43
S/MMA	214	67.82	1.61

[a] The copolymer period was calculated from an empirical formula derived by Anastasiadis et al.[27] δ is the "degree of commensurability", a ratio of the copolymer bulk period to the average substrate stripe periodicity of 42 nm.

morphology normal to the surface and in the stripe direction and, if so, how far into the bulk of the film such an oriented morphology will propagate. Additionally, the commensurability of length scales between the copolymer period and the substrate pattern is examined, and the results are then compared to the case of ultrathin confined films described previously.[15] Finally, the role of ordering kinetics and its influence on the propagation of a surface directed morphology into the bulk region of the films are discussed.

Experimental Section

Symmetric diblock copolymers of P(S-*b*-MMA) were purchased from Polymer Labs or synthesized in-house. All of the copolymers were Soxhlet extracted in cyclohexane to remove any residual polystyrene homopolymer. The molecular weights of the copolymers, the calculated bulk copolymer period,[27] and degree of commensurability (δ) for each copolymer are shown in Table 1. δ is the ratio of the bulk lamellar period of the copolymer to the stripe period of the heterogeneous substrate, 42 nm. Solutions of 5 wt % polymer in HPLC grade toluene were prepared.

Chemically heterogeneous substrates were prepared by glancing angle metal evaporation on facetted Si substrates. Si (113) substrates miscut 1.1° toward the (−1−10) pole were resistively heated and cleaned under ultrahigh-vacuum (UHV) conditions by cycling the surface temperature between 1000 and 1523 °C. Surfaces were then annealed for 100 s at 1180 °C to produce facets of 42 nm average periodicity, with an 8 nm standard deviation and less than 1 nm amplitude. The general processing conditions are described elsewhere.[28] Figure 1a shows an AFM height image of such a surface. These surfaces were then mounted in a thermal evaporator with a 4° angle between the metal source normal and the surface parallel, so that the evaporated metal atoms were incident only on the facing edge of the facets. 1.5 nm of chromium was evaporated initially as an adhesion layer, followed by 2.5 nm of gold (Au), producing a striped, chemically heterogeneous surface with 4.5 nm roughness, as shown in Figure 1b. A simple calculation shows that this roughness is too small to perturb the morphology of the block copolymer.[29] Consequently, the surface is essentially a flat, striped surface with alternating polar oxide and nonpolar gold lines of slightly asymmetric widths. The gold lines are narrower, of order 20 nm, but an exact width is not measurable due to the radius of curvature limitations of the AFM tip. New substrates were prepared for each experiment, as the destructive characterization techniques prevented substrate reuse.

Solution casting was done in a closed glass crystallization dish in the presence of excess solvent, in an effort to control the rate of solvent evaporation and promote an equilibrium morphology.[5] Small substrates (0.25 cm^2) were placed within a 600 mL aluminum foil covered glass crystallization dish. Inside the casting container was an additional small dish filled with toluene, to saturate the vapor pressure inside and mediate solvent evaporation from the substrate. A small, 0.3 cm^2 hole in the foil covering allowed for the deposition of the polymer solution on the substrate via syringe, as well as controlled evaporation. The small substrates were covered entirely with a 5 μL droplet, such that the surface was completely wet but the solution did not spill over the substrate edge. The solvent evaporated completely over the course of 30 min, producing a transparent film of nonunifom thickness. The surface roughness of the films was found to increase with increasing polymer molecular weight, indicating a kinetic limitation in control over the free surface morphology upon solvent evaporation.[30,31]

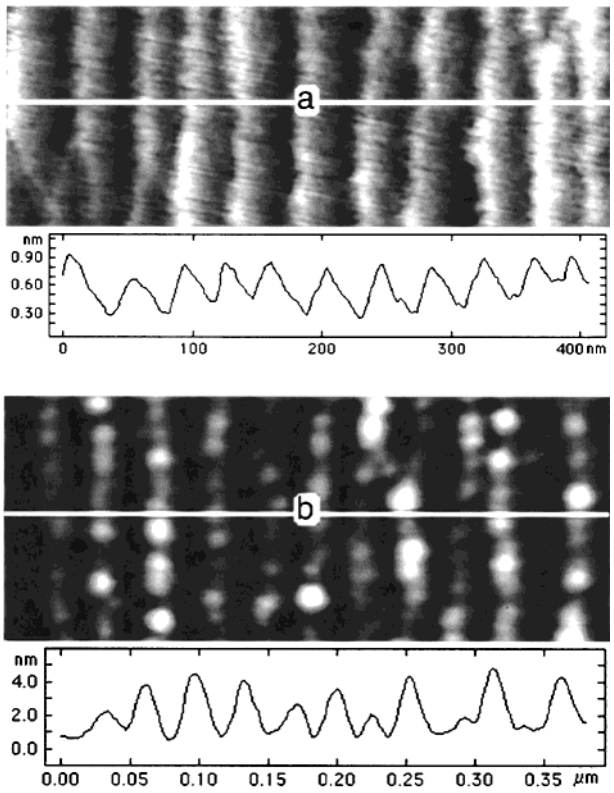

Figure 1. Tapping mode atomic force microscope height images of the topography of 42 nm substrates (a) before and (b) after metallization.

Characterization of the solution cast polymer films was done by field emission scanning electron microscopy (FESEM) on a JEOL 6320. Cast films were first annealed at 190 °C for 2 days to promote relaxation of the polymer film and improve adhesion. This proved necessary to prevent film cracking and delamination from the substrate during cryofracture. The backside of the samples was then scored with a diamond scribe either parallel or perpendicular to the surface striping and submerged in liquid nitrogen for 45 s with knife-edged pliers aligned with the scribe line. Gripping pressure on the pliers would cause the substrate to cleave along the scribe line, producing two facing cross sections. Sections were mounted edge-up on an aluminum FESEM mount with carbon tape. To enhance the topography of the fracture surface, tetrafluoromethane (CF_4) reactive ion etching (RIE) was used. The inherent directionality and etch contrast between PS and PMMA in CF_4 RIE allowed for the development of a material-dependent topography on the fracture surfaces after a brief, low-power etch (25 W, 10 sccm CF_4, 15 mTorr, 2 min).[32−34] Finally, a 20 nm plasma deposited gold coating was applied to the sample, and the FESEM produced crisp images of PS lamellar microdomains in relief from the cross sections.

Results and Discussion

FESEM images of a 107K P(S-*b*-MMA) film solution cast on homogeneous Au and SiOx surfaces are shown

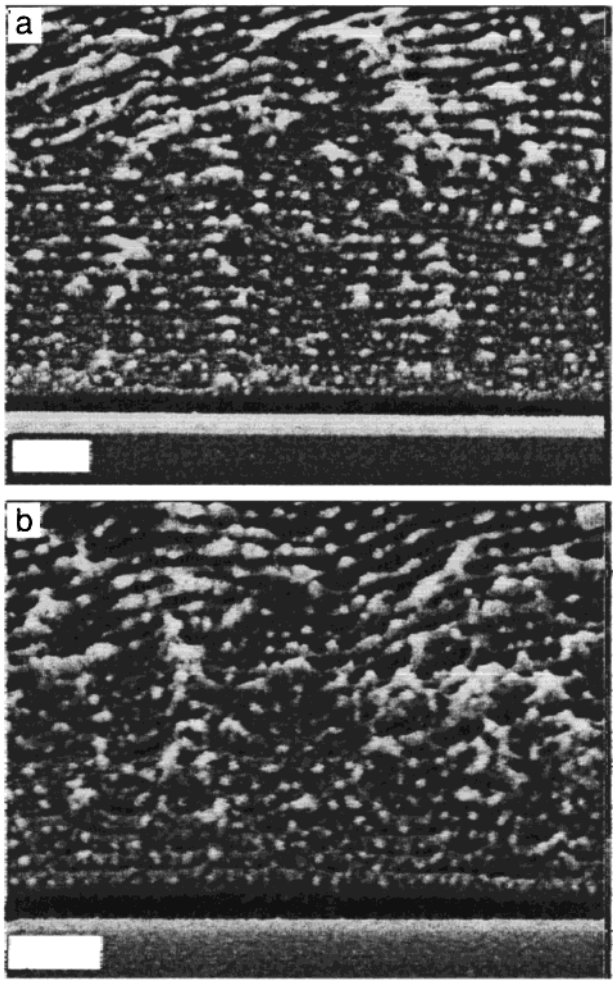

Figure 2. FESEM images of the fracture cross sections of 107K films solution cast on homogeneous surfaces: (a) gold surface, (b) silicon oxide surface. The lamellar morphology of the copolymer is clearly visible, oriented parallel to the substrate. Scale bars are 0.2 μm.

in Figure 2. The two substrates can be distinguished by the appearance of the polymer/substrate interface. The presence of the bright 50 nm thick line at the polymer/Au/Si interface results from the uniform metallization of the substrate by the Au. The dark gap appearing at the polymer/Si interface of the homogeneous Si substrate is caused by electron beam damage. PMMA is rapidly degraded in the electron beam, which results in an adhesive failure at the interface and a pulling of the film away from the surface. This delamination was not seen at the polymer/Au interface due to the presence of a more robust PS wetting layer. The lamellar morphology, however, is seen to be oriented parallel to the substrate regardless of surface chemistry. For all molecular weights over 84K, a similar morphology is observed. For the lower molecular weight copolymers, the cryofracture/RIE imaging technique was unsuccessful, due possibly to the broadness of interface between the PS and PMMA microdomains and resulting lack of RIE etch specificity.

The distance over which the surface directed parallel orientation propagates into the bulk for samples cast on homogeneous substrates is largest for the lower molecular weight samples, averaging 0.5 μm or 12 periods. The highest molecular weight samples show only one or two lamellar layers parallel to the interface before losing orientation. Additionally, the apparent grain size both parallel and perpendicular to the lamellar stacking direction decreases with increasing molecular weight in a similar fashion. In all cases the distance over which the surface-directed morphology propagates away from the surface is less than or equal to the apparent bulk grain size. These results therefore indicate that the generation of a surface-directed morphology upon solution casting is a kinetically limited process. The chain mobility is significantly reduced for the higher molecular weight samples preventing coarsening of the grains, producing shorter correlation lengths.

The FESEM images of a selected molecular weight range from 84K to 177K P(S-*b*-MMA) solution cast on 42 nm Au/SiOx heterogeneous surfaces are shown in Figure 3. The substrates were fractured perpendicular to the surface striping. As molecular weight is increased, the orientation of the lamellar morphology is seen to change from parallel to perpendicular and back to parallel to the surface. For the 107K copolymer, the calculated period is nearly commensurate with the surface pattern with a δ of 1.03. The surface-directed ordering is almost perfect, with few defects seen. The morphology propagates approximately 0.5 μm into the bulk, similar to the propagation length of the parallel morphology on a homogeneous surface. These results suggest that segregation of the copolymer chains to the interface and templating by the striped surface occur prior to the onset of microphase separation. With the PMMA block adsorbed to the oxide and PS onto the gold, the copolymer chains lay parallel to the surface and in registry with the stripes. The segregation at the interface drives the lamellar morphology normal to the substrate into the bulk. For the incommensurate molecular weights, surface segregation does not occur in a controlled, periodic fashion. The entropic penalty associated with straining the copolymer chains to alter the period to match that of the substrate outweighs the enthalpic gains arising from satisfying interfacial interactions. Therefore, a preference develops at the substrate for a single component, either PS or PMMA, and a parallel morphology is driven into the bulk. Tilting of the microdomains with respect to the surface normal, a theoretically proposed intermediate morphology for slightly incommensurate phases,[26] was not observed either. The surface-directed ordering, whether initially parallel or perpendicular to the substrate, propagates only far enough into the bulk to meet the phase-separated grains formed there. There is no evidence that either orientation has a stronger influence on the propagation distance, indicating that kinetics limit the development of the surface-directed morphologies.

The sensitivity of surface-directed orientation to the commensurability between the substrate and copolymer periods in thick films is seen in the 113K P(S-*b*-MMA) sample. In this case $\delta = 1.07$, and a perpendicular lamellar ordering rich with defects is found. The primary defect mode is shown on the far right of the image in Figure 3c. The light striping due to the metallization of the PS lamellae appears to increase abruptly in periodicity. This arises from a reorientation of the lamellae such that they remain perpendicular to the surface but are no longer aligned with the substrate pattern. This "reoriented grain" defect structure was also observed in ultrathin films,[15] where it dominated the morphology for incommensurate systems where $\delta > 1$. Reoriented perpendicular lamellar grain defects

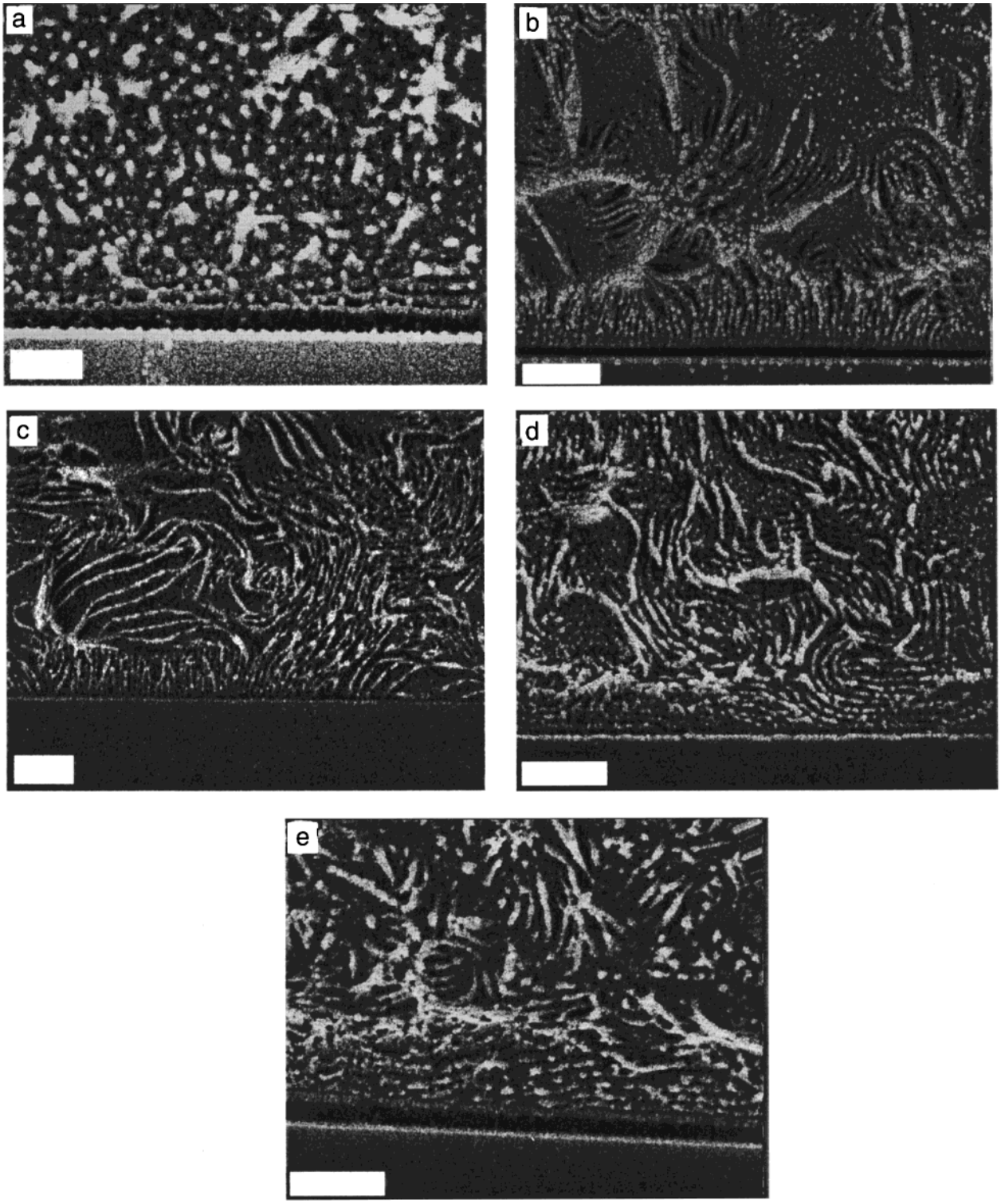

Figure 3. FESEM images of the fracture cross sections of films solution cast on 42 nm Au/SiOx heterogeneous surfaces. Substrates were fractured transversely to the surface striping. (a) 84K (0.2 μm scale bar), (b) 107K (0.5 μm), (c) 113K (0.5 μm), (d) 121K (0.5 μm), (e) 177K (0.5 μm). Parallel lamellar morphologies are evident at the interface for 84K, 121K, and 177K, while perpendicular morphologies are evident for 107K and 113K.

were also seen in the calculations of Chen and Chakrabarti[22] and the simulations of Wang et al.[25] In the former work, defects were apparent when $\delta = 0.667$ at a film thickness equivalent to the copolymer period, while for the latter "$|||^T$", or transposed perpendicular lamellae, were seen originating at the substrate for $\delta = 1.5-3$.

A further increase in molecular weight to 121K ($\delta = 1.11$, Figure 3d) results in a parallel orientation of the lamellae, with no evidence of surface-directed perpendicular ordering. All of the higher molecular weight copolymer films possess a parallel orientation at the substrate as well. As parallel ordering is seen for the lower molecular weight copolymer (84K) with $\delta = 0.88$, it is clear that for thick films a 10% mismatch between copolymer period and surface pattern is sufficient to disrupt a surface directed perpendicular lamellar phase. This window of commensurability is much narrower

than that seen for ultrathin films, where a lamellar morphology oriented normal to the substrate and aligned with the stripes was found when $0.75 < \delta < 1.25$. For the ultrathin films, however, confinement of the morphology by the film thickness promotes an orientation of the lamellae normal to the surface, even in the incommensurate samples.[11,35] Thus, the patterned substrate chemistry need only direct the reoriented ultrathin film morphology in the slightly incommensurate cases, producing an apparently wider window of commensurability. With thick films, confinement effects have been eliminated, and substrate patterning alone is responsible for reorienting the copolymer morphology at the interface.

Under no circumstances was the lamellar morphology found to orient normal to the surface with a random, lateral orientation of the grains. Such a structure would be found if the substrate was effectively "neutral" with respect to its interaction with the copolymer chains.[36] This may arise when the substrate period is much smaller than that of the copolymer, $\delta \gg 1$. The orientation of the lamellar microdomains found for the higher molecular weight copolymers, however, indicates that the heterogeneous substrates are not explicitly neutral toward the copolymers despite the more rapidly alternating chemistry. While limitations of the FESEM characterization technique prohibit explicit identification of a wetting layer at the substrate, the lack of delamination arising from election beam degradation of the PMMA microdomains in the higher molecular weight copolymers indicates a PS wetting layer on all heterogeneous substrates similar to that seen on the homogeneous gold surface in Figure 2.

Confirmation of our description of the lamellar morphologies in Figure 3b,c for 107K and 113K copolymers can be obtained by cryofracturing the substrates parallel to the striping. If the lamellar ordering at the surface were truly perpendicular to the substrate and aligned with the stripes, then the parallel fracture surface would be devoid of any structure at the interface, yet in the bulk show lamellar grains. Figure 4 shows a fracture surface parallel to the stripe pattern for 107K and 113K. For the 107K sample, no structure is evident at the interface. In the bulk, however, microns from the surface, different lamellar orientations are seen. For the 113K sample, evidence of lamellae oriented normal to the surface aligned both parallel and perpendicular to the fracture plane (stripe direction) is seen. This particular image was chosen to exemplify the mixed perpendicular morhphology that can develop due to reoriented grain defects. Increasing or decreasing molecular weight past the 10% commensurability window yields a parallel lamellar morphology in this fracture direction as well.

Conclusion

We have shown that, by patterning a substrate with the appropriate chemistry and length scale, a template to direct the ordering and orientation of block copolymer lamellar morphologies into the film bulk can be made. Striped surfaces of nonpolar gold and polar silicon oxide with 42 nm periodicity guide the growth and ordering of P(S-*b*-MMA). For films greater than 5 μm thickness, commensurability is found to be a key factor in generating surface-directed morphologies. Copolymer films with a bulk lamellar period nearly equal to that of the substrate follow the substrate pattern upon solution casting and orient perpendicular to the interface. When the mismatch is greater than only 10%, the lamellar microdomains orient parallel to the surface. In all cases, kinetics limit the distance over which the structure propagates into the bulk. An increase in molecular weight results in a reduction in mobility, grain size, and the distance over which surface-directed morphologies propagate into the bulk.

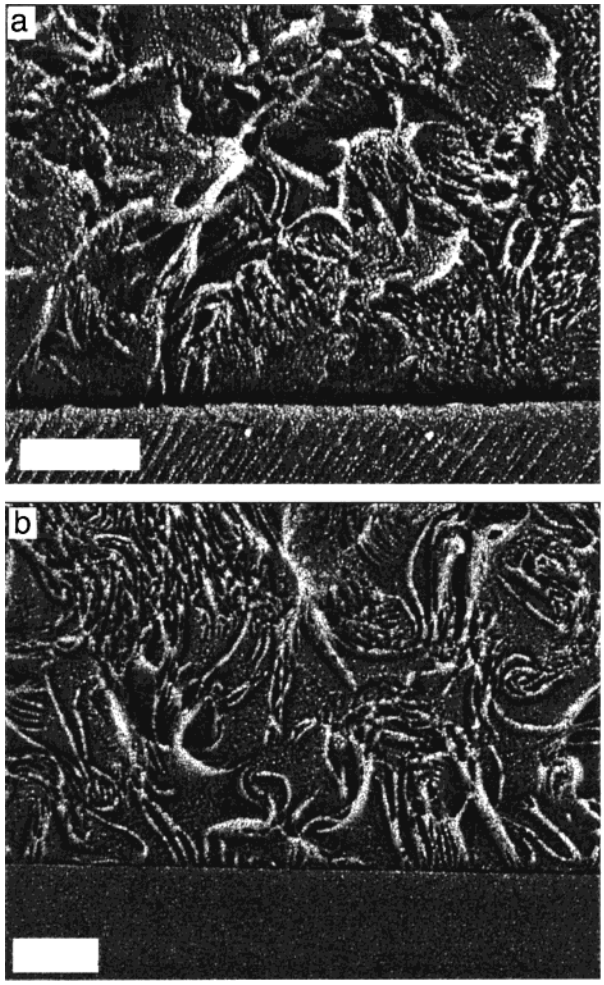

Figure 4. FESEM images of the fracture cross sections of films solution cast on 42 nm Au/SiOx heterogeneous surfaces. Substrates were fractured parallel to surface striping. (a) 107K, (b) 113K. Scale bars are 1 μm.

Acknowledgment. These studies were supported by the National Science Foundation Materials Research Science and Engineering Center at the University of Massachusetts at Amherst, The Department of Energy, Office of Basic Energy Sciences, and NETI. The authors thank Christopher Stafford for assistance with synthesis and characterization of block copolymers, Larry Lurio and Harold Gibson at Argonne National Labs and Mirang Yoon for assistance in facetted silicon preparation, and Louis Raboin for assistance with FESEM experiments.

References and Notes

(1) Harrison, C.; Park, M.; Chaikin, P. M.; Register, R. A.; Adamson, D. H. *J. Vac. Sci. Technol. B* **1998**, *16*, 544−552.
(2) Chan, V. Z.-H.; Hoffman, J.; Lee, V. Y.; Iatrou, H.; Avgeropolous, A.; Hadjichristidis, N.; Miller, R. D.; Thomas, E. L. *Science* **1999**, *286*, 1716−1719.
(3) Lammertink, R. G. H.; Hempenius, M. A.; van den Enk, J. E.; Chan, V. Z.-H.; Thomas, E. L.; Vansco, G. J. *Adv. Mater.* **2000**, *12*, 98−102.

(4) Garetz, B. A.; Balsara, N. P.; Dai, H. J.; Wang, Z.; Newstein, M. C.; Majumdar, B. *Macromolecules* **1996**, *29*, 4675−4679.
(5) Kim, G.; Libera, M. *Macromolecules* **1998**, *31*, 2569−2577.
(6) Russell, T. P.; Coulon, G.; Deline, V. R.; Miller, D. C. *Macromolecules* **1989**, *22*, 4600−4606.
(7) Mansky, P.; Russell, T. P.; Hawker, C. J.; Mays, J.; Cook, D. C.; Satija, S. K. *Phys. Rev. Lett.* **1997**, *79*, 237−240.
(8) Walton, D. G.; Kellogg, G. J.; Mayes, A. M.; Lambooy, P.; Russell, T. P. *Macromolecules* **1994**, *27*, 6225−6228.
(9) Henkee, C. S.; Thomas, E. L.; Fetters, L. J. *J. Mater. Sci.* **1988**, *23*, 1685−1694.
(10) Koneripalli, N.; Levicky, R.; Bates, F. S.; Ankner, J.; Kaiser, H.; Satija, S. K. *Langmuir* **1996**, *12*, 6681−6690.
(11) Fasolka, M. J.; Banerjee, P.; Mayes, A. M.; Pickett, G.; Balazs, A. C. *Macromolecules* **2000**, *33*, 5702−5712.
(12) Coulon, G.; Daillant, J.; Collin, B.; Benattar, J. J.; Gallot, Y. *Macromolecules* **1993**, *26*, 1582−1589.
(13) Lambooy, P.; Russell, T. P.; Kellogg, G. J.; Mayes, A. M.; Gallagher, P. D.; Satija, S. K. *Phys. Rev. Lett.* **1994**, *72*, 2899−2902.
(14) Heier, J.; Kramer, E. J.; Walheim, S.; Krausch, G. *Macromolecules* **1997**, *30*, 6610−6614.
(15) Rockford, L.; Liu, Y.; Mansky, P.; Russell, T. P.; Yoon, M.; Mochrie, S. G. J. *Phys. Rev. Lett.* **1999**, *82*, 2602−2605.
(16) Fasolka, M. J.; Harris, D. J.; Mayes, A. M.; Yoon, M.; Mochrie, S. G. J. *Phys. Rev. Lett.* **1997**, *79*, 3018−3021.
(17) Reiter, G.; Castelein, G.; Hoerner, P.; Riess, G.; Blumen, A.; Sommer, J.-U. *Phys. Rev. Lett.* **1999**, *83*, 3844−3847.
(18) De Rosa, C.; Cheolmin, P.; Thomas, E. L.; Lotz, B. *Nature* **2000**, *405*, 433−437.
(19) Pereira, G. G.; Williams, D. R. M. *Phys. Rev. Lett.* **1998**, *80*, 2849−2852.
(20) Petera, D.; Muthukumar, M. *J. Chem. Phys.* **1997**, *107*, 9640.
(21) Halperin, A.; Sommer, J. U.; Daoud, M. *Europhys. Lett.* **1995**, *29*, 297−302.
(22) Chen, H.; Chakrabarti, A. *J. Chem. Phys.* **1998**, *108*, 6897−6905.
(23) Chakrabarti, A.; Chen, H. *J. Polym. Sci., Part B* **1998**, *36*, 3127−3136.
(24) Wang, Q.; Nath, S. K.; Graham, M. D.; Nealey, P. F.; de Pablo, J. J. *J. Chem. Phys.* **2000**, *112*, 9996−10010.
(25) Wang, Q.; Yan, Q.; Nealey, P. F.; de Pablo, J. J. *Macromolecules* **2000**, *33*, 4512−4525.
(26) Petera, D.; Muthukumar, M. *J. Chem. Phys.* **1998**, *109*, 5101−5107.
(27) Anastasiadis, S. H.; Russell, T. P.; Satija, S. K.; Majkrzak, C. F. *J. Chem. Phys.* **1990**, *92*, 5677−5691.
(28) Mochrie, S. G. J.; Song, S.; Yoon, M.; Abernathy, D. L.; Stephenson, G. B. *Phys. B: Condens. Matter* **1996**, *221*, 105−125.
(29) Pickett, G. T.; Witten, T. A.; Nagel, S. R. *Macromolecules* **1993**, *26*, 3194−3199.
(30) Kim, G.; Libera, M. *Macromolecules* **1998**, *31*, 2670−2672.
(31) Green, P. F.; Christensen, T. M.; Russell, T. P.; Jerome, R. *Macromolecules* **1989**, *22*, 2189−2194.
(32) Huang, E.; Russell, T. P.; Harrison, C.; Chaikin, P. M.; Register, R. E.; Hawker, C. J.; Mays, J. *Macromolecules* **1998**, *31*, 7641−7650.
(33) Harada, K. *J. Appl. Polym. Sci.* **1981**, *26*, 1961−1973.
(34) Harrison, C.; Park, M.; Chaikin, P. M.; Register, R. A.; Adamson, D. H.; Yao, N. Preprint, 1997.
(35) Pickett, G. T.; Balazs, A. C. *Macromolecules* **1997**, *30*, 3097−3103.
(36) Huang, E.; Rockford, L.; Russell, T. P.; Hawker, C. J. *Nature* **1998**, *395*, 757−758.

MA001747C